Batch filtration model of proanthocyanidins purification process from sorghum pericarp extract using polyethersulfone membrane

Moh. Azhar Afandy[1], Wahyudi Budi Sediawan[2,*], Muslikhin Hidayat[2], Devi Yuni Susanti[3], Fikrah Dian Indrawati Sawali[1], Mega Mustikaningrum[4]

[1]Mineral Chemical Engineering. Politeknik Industri Logam Morowali. Jl Trans Sulawesi Desa Labota, Morowali, 94974, Indonesia
[2]Department of Chemical Engineering. Engineering Faculty. Universitas Gadjah Mada. Jl Grafika No. 2 Kampus UGM, Yogyakarta, 55281, Indonesia
[3]Departement of Agricultural and Biosystem Engineering. Agricultural Technology Faculty. Universitas Gadjah Mada. Jl Flora 1. Bulaksumur, Yogyakarta, 55281, Indonesia
[4]Department of Chemical Engineering, Engineering Faculty. Universitas Muhammadiyah Gresik. Jl. Sumatera No. 101 GKB Gresik, 61121, Indonesia
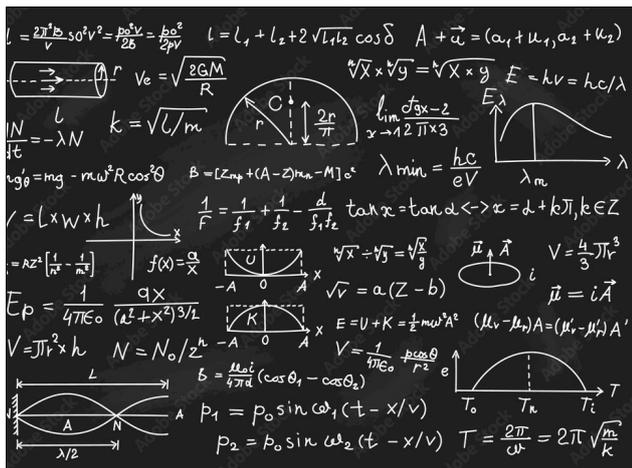
OBJECTIVES The goal of this research is to construct a filtration equation model for the purification of proanthocyanidin compounds in sorghum pericarp extract using the ultrafiltration technique at varied transmembrane pressures (TMP) and molecular weight cut-off (MWCO) on asymmetric polyethersulfone (PES) membranes. The pressure difference and MWCO size are utilized to assess the rate of cake formation induced by fouling and concentration polarization. **METHODS** The model provided in this work is based on a compressible filtration model, which can reflect the reduction in permeability values and the cake formation process induced by the compression of particles deposited on the membrane surface. Hermia's models were used to investigate fouling mechanism involved in UF of proanthocyanidins. **RESULTS** The results demonstrate that transmembrane pressure and MWCO considerably impact the efficacy of the proanthocyanidins separation process employing ultrafiltration membrane technology. The batch filtering model described in this study demonstrates fairly excellent applicability. This can be observed from the data values predicted using the model, which tend to be near to the experimental data

values, with sum square error (SSE) values of 0.3855-0.9965 for PES 50 kDa, 0.0472-0.4365 for PES 30 kDa, and 0.2887-0.5734 for PES 10 kDa. **CONCLUSIONS** The results demonstrated that the best fit to fouling mechanism experimental data using Hermia's model corresponds to the cake layer formation model ($R^2 > 0.99$), followed by the standard blocking model, intermediate blocking, and complete blocking for all the experimental conditions investigated.

KEYWORDS filtration models; membrane; proanthocyanidins; ultrafiltration

1. INTRODUCTION

The pharmaceutical and food sectors are incredibly interested in extracting, purifying, and concentrating high-added-value chemicals from natural sources such as sorghum (Madrona et al. 2019; Víctor-Ortega et al. 2017). Sorghum is the world's fifth-most valued cereal crop, representing less than wheat, rice, maize, and barley. Sorghum is commonly farmed in semi-arid and dry locations, where sorghum porridge is a vital component of the diet due to its drought tolerance and high temperatures (Stefoska-Needham et al. 2015). Sorghum has long been recognized as a helpful plant due to its high polyphenol content. Sorghum polyphenol chemicals may be antioxidants for human health (Wu et al. 2017). Phenolic chemicals in sorghum include phenolic acids, proanthocyanidins, 3-deoxy anthocyanidins, and flavonoids (Anderson et al. 2012; Barros et al. 2014; Chiremba et al. 2012; Lee et al. 2014; Massey et al. 2014). Sorghum's total polyphenol concentration is controlled by genetic and environmental variables such as plant colors, pericarp thickness, and growing circumstances (Svensson et al. 2010).

Condensed tannins, commonly known as proanthocyanidins, are the most prevalent polyphenols in sorghums with a colored test (Barros et al. 2014). Sorghum has the largest tannin concentration of any crop, with high molecu-

lar weight proanthocyanidin being the most prevalent (Dykes and Rooney 2007; Hagerman and Butler 1980). As an end product of the flavonoid biosynthetic pathway, proanthocyanidins are oligo- or polymers of monomeric flavan-3-ols. Proanthocyanidins are condensed tannins formed by the action of a multi-enzyme complex in the cytosol along the phenylpropanoid pathway. The average number of proanthocyanidin was 1500-5000 depends on its polimer structure (Czochanska et al. 1980). The proanthocyanidin content in sorghum depends on the genetic and environmental variables that regulate tannin biosynthesis (Wu et al. 2012). According to the study by Susanti et al. (2021), the proanthocyanidin level in sorghum was 9.113–9.227 mg/g. Proanthocyanidins are renowned for their significant chemical and biological activities, including UV absorption, antibacterial, antioxidant, anti-cancer, and nerve protection (Rauf et al. 2019). Another study by Ratnavathi and Tonapi (2021). reported that the total proanthocyanidin content of black sorghum bran was 0.9 mg/g, while red and brown sorghum brans had 0.2 mg/g and 0.1 mg/g. previous research by Mora et al. (2022) reported that the amount of (+)-catechin, a proanthocyanidin, in some sorghum varieties ranges from 172 to 179 mg/100 g.

Membranes have become an essential component of biotechnology, and advances in membrane technology are now aimed at achieving higher bioproduct resolutions (Asif et al. 2018). Membrane technology is increasingly being used in both upstream and downstream technologies, such as microfiltration (MF), ultrafiltration (UF), and emerging methods such as membrane chromatography, high-performance tangential flow filtration, and electrophoretic membrane contactors (Arribas et al. 2015; Córdova et al. 2018; Favre 2022; Mejia et al. 2022; Rajendran et al. 2021; Raza et al. 2019). Membrane technology is one of the option separation methods used in global industries (Purwayantie and Sediawan 2020). According to previous research, membrane technology can be used to separate and purify polyphenol compounds (Cassano et al. 2018; Conidi et al. 2017, 2018; Madrona et al. 2019; Nawaz et al. 2006; Rodrigues et al. 2020; Víctor-Ortega et al. 2017). Membrane filtration has several advantages over conventional separation and purification processes, including high efficiency, superficial modification of operating variables, and low energy requirements, and a suitable option for fruit or plant extract treatment because it is done at low temperatures and preserves the food's functional nutrients while using little energy (Chen et al. 2020; Madrona et al. 2019). Several types of membranes commonly used in the separation of phenolic compounds by the UF process include Polyethersulfone (PES), polyvinylidene difluoride (PVDF), and Polysulfone (PS) (Ambarita et al. 2021; Fan et al. 2016; Wen et al. 2022). According to previous research by Mejia et al. (2022), PES membranes can be utilized for the recovery and separation of polyphenolic components and polysaccharides from Sangiovese and Cabernet Sauvignon wines. The results indicated that all PES UF and NF membranes successfully separated target chemicals, rejecting more than 92% of polysaccharides, with polyphenols preferentially entering through the membrane. The UF membrane left more than 40% of total polyphenols; rejections toward non-flavonoids and flavonoids were less than 25% and 12.5%, respectively. Another research by Pinto et al. (2017) reported that ultrafiltration and nanofiltration are suitable techniques for the con-

centration of Eucalyptus bark extract, allowing the recovery of valuable polyphenols.

The primary disadvantage of membrane-based separation processes is the decrease in permeate flux during filtration caused by the membrane fouling and concentration polarization (Conidi et al. 2018; Koonani and Amirinejad 2019). Membrane fouling occurs when particles, colloidal particles, or solute macromolecules are deposited or adsorbed onto membrane pores or surfaces through physical and chemical interactions or mechanical action, resulting in smaller or blocked membrane pores (Liu et al. 2018). When the solute concentration at the membrane surface increases, the solute's solubility decreases, and solute precipitation begins to clog the membrane (Darunee Bhongsuwan et al. 2002). Concentration polarization is a process in which retained solutes accumulate at the membrane boundary on the feed side. It is an unavoidable result of membrane selectivity (Ang and Mohammad 2015). With the formation of a cake layer, this phenomenon will cause the membrane to be rejected partially or entirely (Conidi et al. 2018). Controlling both phenomena is critical for the membrane process in industrial applications. Choosing a suitable membrane for phenolic compound ultrafiltration depends on numerous criteria, such as the source of phenolic compounds, initial concentration, molecular size, transmembrane pressure, and membrane properties. The membranes employed should have tiny pores to hold phenolic chemicals and skip water and other undesirable particles. Membranes should also resist fouling, i.e., the collection of chemicals restricting fluid flow across the membrane.

Separation by utilizing membranes is a good choice owing to the concept of such a technique that may separate proanthocyanidin compositions based on the sieving effect principle, in which particles or composites can be divided according to their dimensions by rejecting undesirable substances and permitting the others to pass through the membrane (Afandy et al. 2023; Conidi et al. 2018; Hori and Unno 2011; Malliga et al. 2019; Saleh and Gupta 2016). The method will retain molecules more significant than the membrane hole's size and keep on the membrane surface and feed solution (Zheng et al. 2009). The primary objective of this study was to develop a mathematical model for the filtration process used to purify proanthocyanidins compounds in sorghum pericarp extract. This was achieved by employing an ultrafiltration technique with different transmembrane pressures and molecular weight cut-off sizes on polyethersulfone membranes. Additionally, the study aimed to investigate the fouling mechanism associated with the ultrafiltration processes. The rate of cake formation generated by fouling and concentration polarization is determined by the pressure difference and the molecular weight cut-off (MWCO) of the PES membrane.

2. RESEARCH METHODOLOGY

2.1 Model development

The batch filtration approach is being employed in this investigation. It should be noted that there are two separate approaches for running a batch filter if the pressure stays constant. The flow rate steadily lowers. However, the pressure must progressively increase if the flow rate remains constant (Chhabra and Basavaraj 2019). Cake formation is an is-

sue that must be addressed in a batch filtration mechanism since when too many cakes develop, and the filtration process must be put off to remove the cake so that time is spent effectively at this point. The following equation may compute the connection between laminar and linear velocities at any moment (V) during filter cake development.

$$J = \frac{1}{A}\frac{dV}{dt} = \frac{K(-\blacksquare Pc)}{L\mu} \tag{1}$$

Mass balance:
Mass of solids in cake = mass of solids in slurry

$$(1-X)LA\rho s = \frac{(V + XLA)\rho x}{(1-x)} \tag{2}$$

$$V = \frac{[\rho s(1-x)(1-X)] - \rho xX}{\rho x}AL \tag{3}$$

$$L = \frac{V\rho x}{A[\rho s(1-x)(1-X) - \rho xX]} \tag{4}$$

Equation (3) shows the relationship between filtrate volume (V) and cake thickness (L). which is used to eliminate L in equation (1). so:

$$\frac{dV}{dt} = \frac{KA^2[\rho s(1-x)(1-X) - \rho xX](-\Delta Pc)}{\mu V\rho x} \tag{5}$$

Equation (5) represents the instantaneous rate of filtration in terms of slurry, cake, filtrate amount, and pressure drop through the cake. The variables within the operator's control for a given slurry are pressure drop (-ΔPc). Filtrate volume V. and time t. The cake porosity X is the most likely to alter among the other parameters. Cv is defined by consolidating several components in equation (5) into a single term.

$$Cv = \frac{\mu\rho x}{2K[\rho s(1-x)(1-X) - \rho xX]} \tag{6}$$

$$\frac{dV}{dt} = \frac{A^2(-\Delta Pc)}{2CvV} \tag{7}$$

The above formula applies to zero suppression. But because it employs a filter as a primary filter material. There is pressure from the filter when filtering starts. Suppose the filtrate volume (Ve) is the volume of filtrate accommodated, which induces the creation of a cake. This is comparable to the flow resistance of membrane and filter channels, where
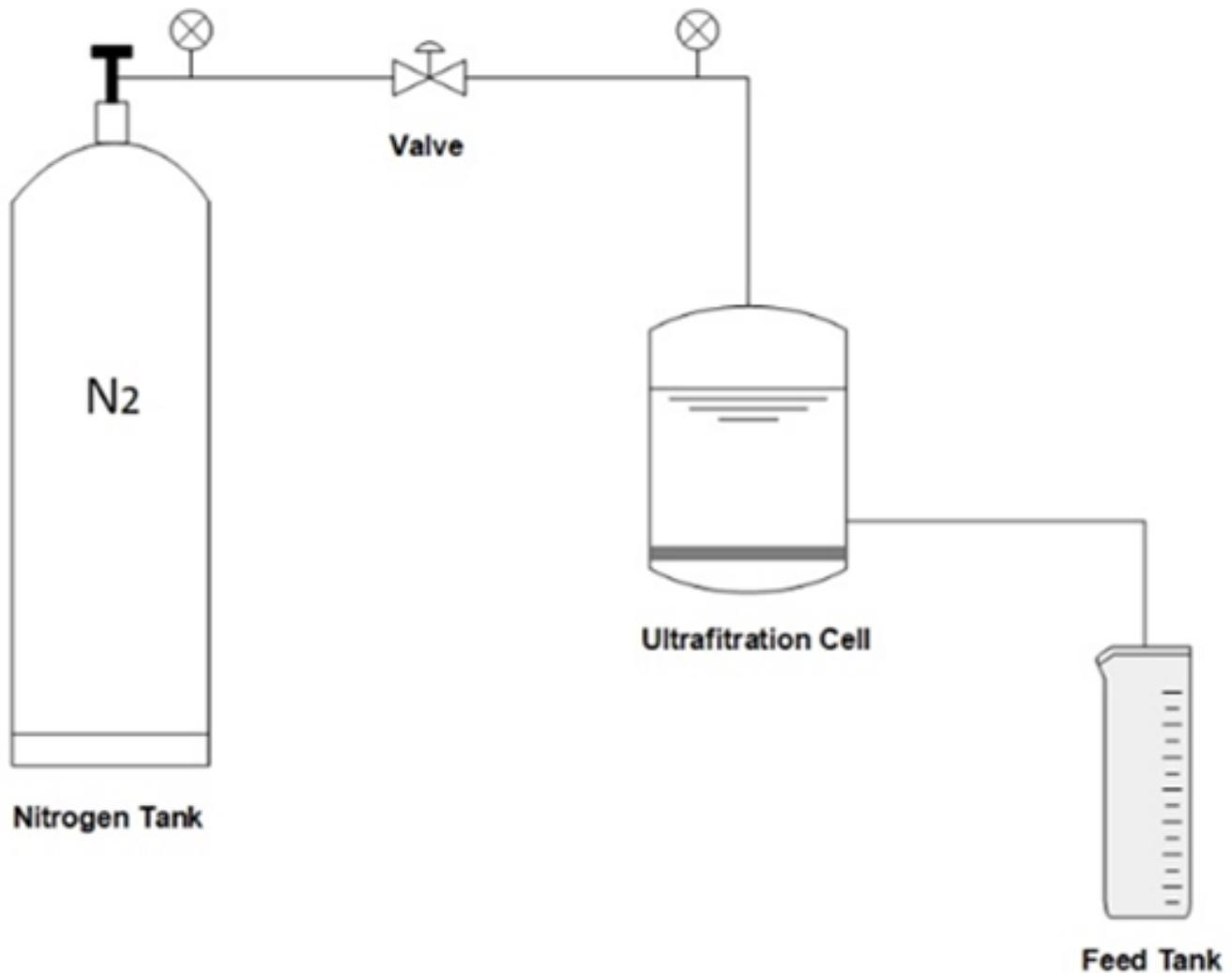
the cake will offer the same pressure as the filter device's suppression. Such that:

$$V \rightarrow V + Ve \qquad (8)$$

then.

$$\frac{dV}{dt} = \frac{A^2(-\Delta Pc)}{2Cv(V + Ve)} \qquad (9)$$

$$\frac{dt}{dV} = \frac{2Cv}{A^2(-\Delta Pc)}(V + Ve) \qquad (10)$$

From this equation. the filtration time is obtained as follows:

$$\int_{t=0}^{t=t} dt = \frac{2Cv}{A^2(-\Delta Pc)} \int_{V=0}^{V=V} (V + Ve)dV \qquad (11)$$

$$t = \frac{Cv}{A^2(-\Delta Pc)}(V^2 + 2VeV) \qquad (12)$$

if:

$$\frac{Cv}{A^2(-\Delta Pc)} = \frac{1}{\alpha} \qquad (13)$$

then obtained:

$$t = \frac{1}{\alpha}(V^2 + 2VeV) \qquad (14)$$

To calculate the value of V. the formula can be described as follows:

$$V = -Ve + \sqrt{Ve^2 + \alpha t} \qquad (15)$$

With:

$$\alpha = \frac{A^2(-\Delta Pc)}{Cv} \qquad (16)$$

2.2 Feed preparation

Sorghum pericarp extract was generated from the extraction of sorghum (Sorghum bicolor L. Moench) from Wonogiri, Indonesia. Then produced by using distilled water as a solvent with a ratio (1:100) at 70°C in a microwave-assisted extraction at 400 rpm of agitation speed for 150 minutes. The extract was then filtered using filter paper.

2.3 UF membrane

This research used an asymmetric Polyethersulfone (PES) membrane supplied by Sartorius Filtrasi Indonesia (Sartorius Stedim Biotech, Germany). Meanwhile, the PES membrane has hydrophobic properties and compatible membrane materials due to their excellent film-forming capabilities and great thermal, chemical, and biological resistance over a wide range of pH (2-12) (Alsvik and Hägg 2013; Lutz 2010; Pabby et al. 2009). The PES membrane has a transpar-

ent and amorphous structure with a high Tg of up to 225°C. According to a study by Rahimpour et al. (2008), the PES membrane has a mean pore size of 50 nm, pore density of 61 pores/μm^2, and surface porosity of 11,2 %. The water contact angle from the PES membrane is 88,6° (Wang et al. 2014).

2.4 Dead-end UF system

This investigation was carried out using the laboratory-scale UF approach. UF membrane separation was performed utilizing the dead-end filtration method with N$_2$ gas as the driving pressure (Afandy et al. 2023). The advantages of dead-end filtering are minimal capital costs, excellent product recovery, and a simple operation. The extract was initially passed through the microfiltration membrane using the 0.2 μm PES membrane at 1 bar of pressure before continuing to the ultrafiltration stage to remove organic materials, bacteria, fungi, yeast, and macromolecules with a higher particle size. First, distilled water was utilized to prepare the PES membrane to eliminate the residual organic material. The ultrafiltration step was carried out with three distinct Molecular weight cut-offs (MWCO) of PES membranes and varied transmembrane pressures (TMP) throughout the operation. Each with a MWCO of 50 kDa (TMP = 2-4 bars). 30 kDa (TMP = 4-6 bars). And 10 kDa (TMP = 8–10 bars). Membrane replacement was carried out in each step. The MWCO was chosen according to proanthocyanidin's molecular weight. Based on earlier research, the impacts of TMP and MWCO considerably influence the filtrate volume (Abolore et al. 2010; Md Yunos et al. 2019; Rai et al. 2006; Syahputri et al. 2021).

2.4.1 Filtrate volume

The permeation flow rate from the UF stage can be predicted based on the modeling results using the batch filtration model equation. The data were collected every 20 minutes for 2 h using a measuring cylinder. The permeation flow rate could be determined based on the relationship between permeation volume and operation time by employing Eq. (9).

$$\frac{dV}{dt} = \frac{A^2(-\Delta Pc)}{2Cv(V + Ve)}$$

2.4.2 Fouling mechanism

To identify the fouling mechanism that occurs in the proanthocyanidin purification process using PES UF membranes, can use the Hermia's model, which describes a semi-empirical model for dead-end filtration based on constant pressure conditions, to estimate the fouling mechanism that influences the flux decreases (Zhu et al. 2015). The Hermia's Models use constant pressure filtration rules for dead-end filtration from Eq (17).

$$\frac{d^2t}{dV^2} = k\left(\frac{dt}{dV}\right)^n \qquad (17)$$

According to Vela et al. (2008), there are four primary forms of fouling: the complete blocking model, the intermediate blocking model, the standard blocking model, and the cake layer model. The fouling process may be defined by fitting the flux data by comparing the coefficient of correlation (R^2) using linear regression.
for n=2 (complete blocking):

TABLE 1. Coefficient R^2 of filtration blocking model for different PES Membrane.

MWCO (kDa)	TMP (Bar)	Complete blocking	Standard blocking	Intermediate blocking	Cake formation layer
	2	0.9717	0.9896	0.9818	0.9986
	2.5	0.9717	0.9896	0.9818	0.9986
50	3	0.9649	0.9875	0.9776	0.9985
	3.5	0.9531	0.9841	0.9707	0.9984
	4	0.9603	0.9861	0.9749	0.9985
	4	0.9171	0.9755	0.9509	0.9987
	4.5	0.8972	0.9718	0.9410	0.9991
30	5	0.9053	0.9732	0.9449	0.9989
	5.5	0.8969	0.9718	0.9408	0.9991
	6	0.8923	0.9711	0.9386	0.9992
	8	0.9423	0.9812	0.9645	0.9985
	8.5	0.9198	0.9760	0.9523	0.9987
10	9	0.9320	0.9787	0.9589	0.9986
	9.5	0.9369	0.9798	0.9615	0.9985
	10	0.9409	0.9808	0.9637	0.9985

$$\ln J = \ln J_0 - K_c t \qquad (18)$$

for n=1.5(standart blocking):

$$\frac{1}{J^{0.5}} = \frac{1}{J^{0.5}} + K_s t \qquad (19)$$

for n=1(intermediate blocking):

$$\frac{1}{J} = \frac{1}{J_0} + K_i t \qquad (20)$$

For n=0 (Cake layer formation):

$$\frac{1}{J^2} = \frac{1}{J_0^2} + K_g t \qquad (21)$$

2.4.3 Models parameter

For compressible cakes, estimating the values of Cv and Ve at different pressure drops and the instantaneous value of V is necessary. The CV value is a constant representing a filtering process that is impacted by the amount of pressure and the surface area of the filter. The equivalent volume (Ve) is the quantity of filtrate included in the filtrate that causes the

development of a cake equivalent to the flow resistance of the membrane and filter channels. The cake layer is an aggregation of substances that cannot penetrate the membrane but remain on its surface. Eqs. (15) and (16) were applied to determine the feed volume at numerous intervals throughout the ultrafiltration membrane process to purify the sorghum pericarp extract.

$$V = -Ve + \sqrt{Ve^2 + \alpha t}$$

With :

$$\alpha = \frac{A^2(-\Delta Pc)}{Cv}$$

2.4.4 Sum Square Error (SSE)

The Sum Square Error (SSE) value refers to the statistical approach used in regression analysis to discover the point of spread of data. It may locate the best-suited function by modifying a small quantity of data. The SSE was computed to establish that the compiled model is based on the non-linear equation of the batch filtering model. The function error value may show a correlation between the model developed and the experimental data, indicating how accurately the observed data is created. The minimal value of SSE implies that the model has been organized properly. The SSE value could be determined using Eq (**??**).

TABLE 2. Hermia's model parameter.

MWCO (kDa)	TMP (Bar)	Kc x 10^{-3} (s^{-1})	Ks x 10^{-3} ($s^{-0.5}m^{-0.5}$)	Ki x 10^{-4}(m^{-1})	Kg x 10^{-4} ($s\ m^{-2}$)
	2	4.08	0.6301	3.9040	0.7563
	2.5	4.08	0.6301	3.9039	0.7537
50	3	4.59	0.6949	4.2211	0.7882
	3.5	5.39	0.7820	4.5676	0.7923
	4	4.92	0.7115	4.1389	0.7102
	4	7.40	1.17	7.5389	1.6084
	4.5	8.34	1.28	8.0317	1.6421
30	5	7.97	1.21	7.4746	1.4799
	5.5	8.35	1.25	7.5726	1.4575
	6	8.56	1.26	7.5542	1.4198
	8	6.05	1.04	7.2031	1.7672
	8.5	7.26	1.21	8.1435	1.9087
10	9	6.62	1.10	7.3409	1.6870
	9.5	6.36	1.06	7.0824	1.6308
	10	6.13	1.01	6.7228	1.5206

$$SSE = \sum_{i=1}^{n} (Vdata - Vcalc)^2$$

3. RESULT AND DISCUSSION

3.1 Effect of TMP on permeation flow rate

One of the factors that became the focus of attention in the ultrafiltration process was the rate permeation flow rate. The permeation flow rate of sorghum pericarp extract using 50 kDa, 30 kDa, and 10 kDa PES membranes are shown in Fig. 2a, 2b, 2c. Such permeation flow rate data shows that higher transmembrane pressure on the process would increase the permeation flow rate. The high transmembrane pressure not only helps the feed to flow through the membrane rapidly and overcome resistance but also promotes the accumulation of substances up to the decrease of the protrusion component, resulting in concentration polarization. According to some research, permeate flux increases by more than 96%, increasing TMP in the 0.25 to 3.0 bar range for ultrafiltration (UF) hollow fiber membranes (Ramli and Bolong 2016). Another study by Conidi et al. (2020) observed that increasing TMP from 0.5 to 2 bar enhanced the permeate flux by 50% and the solute rejection by 10% for UF of phenolic compounds from olive mill wastewater using a 2500 Da membrane. In the application of separation utilizing membranes on an industrial scale, it will be vital to manage such events. The data collected in this investigation was carried out under cir-

cumstances of continuous operating pressure. Thus, maintaining the volume of permeate to remain high can be done by increasing the operating pressure continuously according to the batch filtration model equation, where an increase in pressure will affect the feed volume that will then pass through the membrane.

3.2 Effect of MWCO on permeate volume.

MWCO (molecular weight cut-off) is a metric that shows the size of the most significant molecule that can be passed through the membrane. Permeability is the rate at which fluid flows through the membrane. The effect of MWCO on permeability varies on the type of membrane and fluid employed. In general, the greater the size of the MWCO, the higher the permeability because the membrane pores are more prominent and more accessible for fluids to pass through. However, many additional elements affect permeability, such as the surface charge of the membrane, the transmembrane pressure, and the physicochemical parameters of the fluid (Dillmann et al. 2020). The decrease in permeate flux during the filtration process can be described based on four mechanisms: complete blocking, standard blocking, intermediate blocking, and a cake layer formation on the membrane surface (Conidi et al. 2018). The conclusions presented in Table 1 are based on Hermia's models. The fouling mechanism that happens on PES membranes with sizes
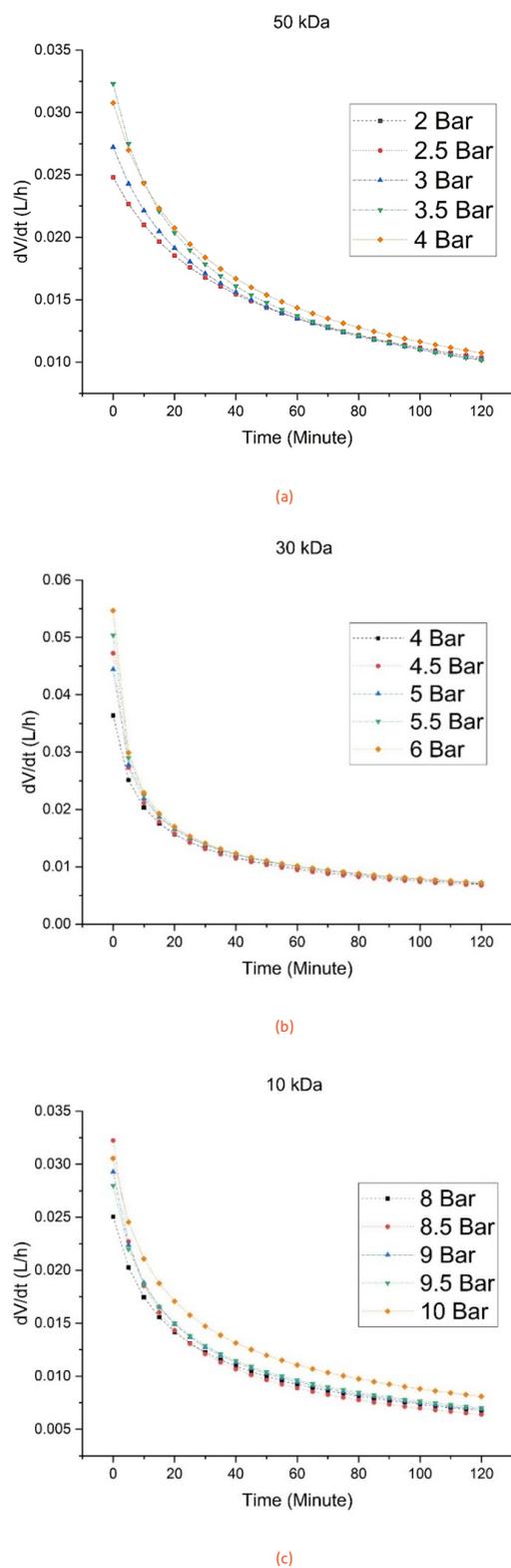
FIGURE 2. Permeation flow rate of Sorghum Pericarp Extract at different MWCO.

of 50, 30, and 10 kDa may be expected to be that the cause of fouling is dominated by the production of a cake layer on the surface of the PES membrane. This may be observed by the R^2 value, which is near to 1. This can occur when the particle size of phenolic compounds, particularly proanthocyanidins, is bigger than the size of the membrane pores and creates a porous cake layer. The thickness of the cake layer is primarily determined by the balance between the rate of

molecule deposition on the membrane surface and the rate of molecule transport back into the bulk solution. The results of evaluation using Hermia's model also demonstrate that the R^2 value for the entire fouling creation mechanism is above 0.9 for each blocking mechanism. According to study done by Bolton et al. (2006) this may be induced by the complicated effect of numerous elements (feed composition, interaction between membrane pore size and molecules in the feed, and membrane material), which generates a mixture of fouling processes during a filtering process.

According to studies by Conidi et al. (2020) reducing MWCO will decrease the permeate flux and improve phenolic compounds' solute rejection. Still, it also increases membrane fouling, which is the buildup of solutes and particles on the membrane surface or pores that limit the permeability and performance of the membrane. Another work from Cai et al. (2018) revealed that decreasing MWCO from 100 to 10 kDa decreased the permeate flux by 80% and increased the solute rejection by 20% for UF of four common polyphenols in model fruit juice using polyethersulfone (PES) membranes. A study by Cassano et al. (2018) revealed that decreasing MWCO from 10 to 1 kDa decreased the permeate flux by 50% and increased the solute rejection by 30% for UF of phenolic components and sugars from artichoke extracts using polyvinylidene fluoride (PVDF) membranes. based on our previous investigations. The rejection coefficients of PES membranes are 25.50–28.18% for PES 50 kDa, 54.50–56.47% for PES 30 kDa, and 80.24–82.74% for PES 10 kDa (Afandy et al. 2023). Based on this, it can be stated that the smaller the pore size of the membrane, the higher the rejection coefficient value of the PES membrane.

The data shown in Table 2 represents the parameter values acquired from Hermia's model while utilizing PES membranes for the purification of proanthocyanidins at different MWCO sizes. A higher value of this parameter signifies an elevated degree of fouling resulting from the fouling mechanism. The fouling process is considered to be caused by the creation of a cake layer on the surface of the PES membrane. The constant value in Hermia's model for cake layer creation, known as Kg, is dependent on the size of the MWCO. As the MWCO size increases, the Kg value also increases because the smaller pores of the membrane lead to a greater creation of a cake layer on its surface. The same phenomenon is illustrated by other parameters in the mechanism of fouling development, specifically the values of Kc, Ks, and Ki. The cake layer can operate as a secondary membrane with a lesser porosity and pore size than the original membrane. The cake layer can cover or change the surface characteristics of the membrane, which impacts the interaction between the membrane and particles and solutes, and the cake layer can contain abrasive, acidic, or alkaline compounds that can damage the structure and integrity of the membrane. Cake formation is a prevalent difficulty in the ultrafiltration of phenolic compounds, which are organic molecules that include one or more hydroxyl groups linked to an aromatic ring. Phenolic chemicals can form a cake layer on the membrane surface due to their high molecular weight, polarity, and inclination to aggregate (Cifuentes-Cabezas et al. 2023; Madrona et al. 2019).

Fouling and concentration polarization both contribute to cake formation (Conidi et al. 2018). Membrane fouling is

the process by which particles, colloidal particles, or solute macromolecules are deposited or adsorbed onto membrane pores or surfaces through physical and chemical interactions or mechanical action, resulting in smaller or blocked membrane pores (Liu et al. 2018). External fouling is the deposition of particles, colloids, and macromolecules on the membrane surface. External fouling causes a fouling layer to form on the membrane's surface. The fouling layer is defined as either a gel layer or a cake layer. Due to the pressure differential between the feed and permeate sides of the membrane, the gel layer is created by the deposition of macromolecules, colloids, and inorganic solutes on the membrane's surface. The cake layer is formed by particles gathering on the membrane surface (Blandin et al. 2016). Concentration polarization refers to the continual passage of polluted influent to the membrane surface and the selective retention of specific elements, which results in the concentration of particular solutes on or near the membrane surface. Their concentration develops throughout the procedure, producing a more significant concentration border layer (Sadr and Saroj 2015).

3.3　Evaluation of parameters from batch filtration models

Several factors revealed that the influence of TMP and MWCO was highly considerable. Related to this, the process parameters need to be examined. A good model is anticipated to correctly forecast the computed volume filtration constant and equivalent volume throughout the dead-end UF process. This mathematical model is performed using Microsoft Excel software, which is utilized to acquire the calculated V, Cv, Ve, and SSE. To begin analyzing these values, compare the Cv and Ve values with estimated values likely to create the slightest inaccuracy. The second step is to compute the value of V using the previously acquired filtering equation. Then calculate the SSE value, the difference between the estimated volume and the data volume squared. The SSE value is then solved using the GRG nonlinear approach to produce the minimal SSE value for each data set. The previously acquired SSE values served as the aim, while the Cv and Ve trial values served as the changing variable cells. The importance of Cv, Ve, and SSE obtained for each membrane is presented in Table 3.

3.4　Models parameter

Based on the data in Table 3, the Cv value produced on a 50 kDa membrane ranges from 17.4001 to 51.4928 cm^2/s. Cv values for a 30 kDa membrane went from 134.8996 to 212.4157 cm^2/s. The obtained Cv values for the 10 kDa membrane ranged from 319.5685 to 397.0216 cm^2/s. The experimental data suggested that the smaller the PES membrane's pore size, or MWCO, the higher the Cv value. This is because the smaller MWCO consumes a more considerable working pressure, boosting the process's Cv value. The amount of pressure significantly influences the Cv value; hence, its value will expand in direct proportion to the rise in operating pressure. The smaller membrane pores size will affect the working pressure as it will enhance the hydrodynamic retention of the membrane. More significant pressure is needed to push water through smaller membrane pores. However, smaller pore sizes can also improve the probability of rejection for pollutants that have a molecular weight more significant than the membrane pore size.
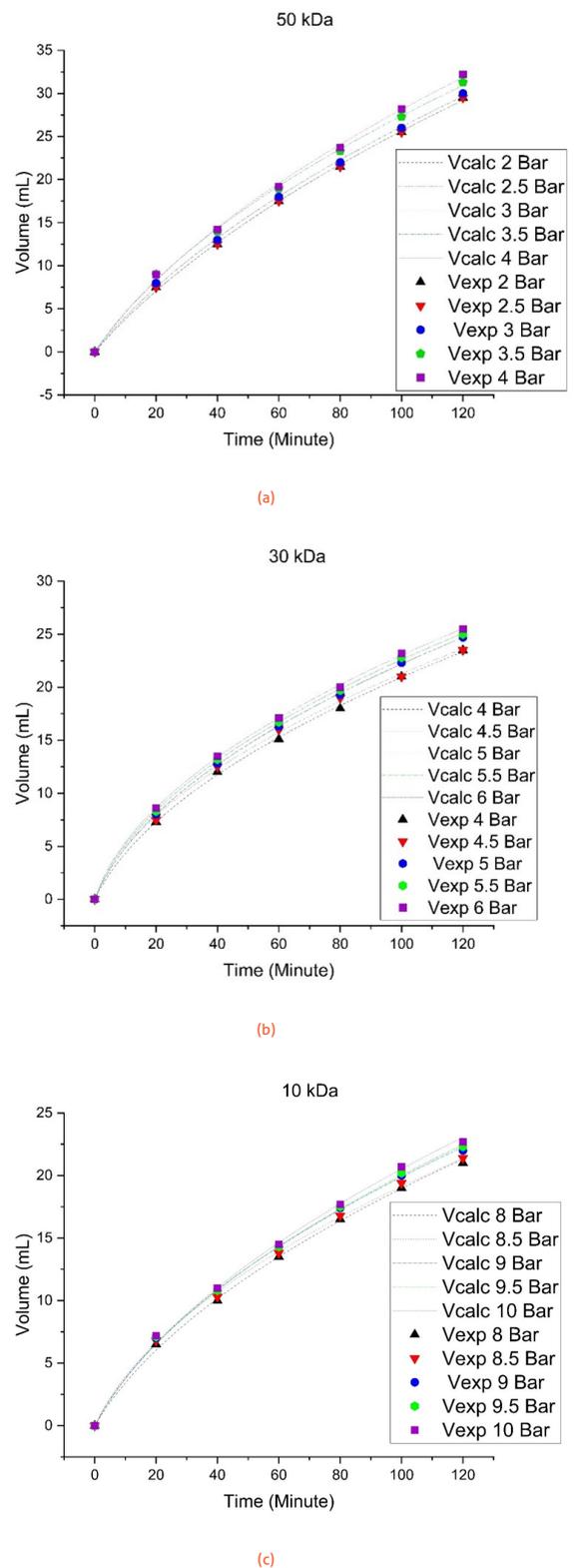

FIGURE 3. Experimental data and Predicted data of Sorghum Pericarp Extract permeate volume at different MWCO 50 kDa, 30 kDa and, 10 kDa.

The information presented in Table 3 reveals that the equivalent volume (Ve) for a 50 kDa membrane is relatively significant. The fastest cake formation occurred on a 50 kDa membrane when the filtrate volume was 14.199 mL at a pressure of 3.5 bar, while the most extended cake formation occurred when the filtrate volume was 20.922 mL at a pressure of 2 bar and 2.5 bar. The quickest cake formation happened on a 30 kDa membrane when the filtrate volume was 3.887

TABLE 3. Value of Cv, Ve, and SSE at different TMP and membrane MWCO.

Membrane MWCO	Pressure (Bar)	Cv (cm^2/s)	Ve (mL)	SSE
	2	17.4001	20.9218	0.3855
	2.5	26.0992	20.9229	0.3855
PES 50 kDa	3	37.3852	17.7432	0.5285
	3.5	49.2273	14.1995	0.8282
	4	51.4928	17.1001	0.9965
	4	134.8996	5.5170	0.1893
	4.5	169.7418	3.9403	0.4365
PES 30 kDa	5	171.0955	4.7496	0.0472
	5.5	193.8752	4.1600	0.0944
	6	212.4157	3.8871	0.1047
	8	319.5685	7.8993	0.3527
	8.5	397.0216	5.2917	0.2887
PES 10 kDa	9	360.5881	6.8424	0.2855
	9.5	364.6573	7.5220	0.4360
	10	355.1995	8.3231	0.5734

mL at a pressure of 6 bar, while the most extended cake formation occurred when the filtrate volume was 5.517 mL at a pressure of 4 bar. The fastest cake formation happened on a 10 kDa membrane when the filtrate volume was 5.292 at 8.5 pressure, whereas the most extended cake formation occurred when the filtrate volume was 8.323 mL at 10 bar.

Based on the values of Ve on each of these membranes, it can be inferred that elevating the transmembrane pressure promotes cake growth on the membrane's surface, which tends to be quicker. Cake growth on the surface of the membrane will affect the performance and efficiency of the membrane in several ways, including reducing the permeate rate by increasing the hydraulic resistance of the permeate flow and reducing the transmembrane pressure, which is the driving force for the ultrafiltration process. Some proposed techniques to prevent or decrease the cake formation on ultrafiltration of phenolic compounds are: raising the velocity of the feed solution parallel to the membrane surface. This can provide a shear force that can limit the accumulation of phenolic compounds on the membrane surface and increase the back-transport of solutes away from the membrane. Adding surfactants, molecules that can reduce the surface tension of liquids and enhance the solubility of phenolic compounds, can avoid the aggregation and precipitation of phenolic compounds on the membrane surface and minimize cake resistance. Adjusting the pH, which measures acidity or alkalinity

in a solution, can influence the charge and solubility of phenolic compounds and their interaction with the membrane surface. A pH near the isoelectric point of the membrane can diminish the electrostatic interaction between the membrane and the phenolic chemicals and reduce cake formation.

3.5 Error analysis

The SSE value (sum square error) found in Table 3 for each membrane is for a 50 kDa membrane; the most negligible error value achieved is 0.3855 at 2 and 2.5 bar pressures, and the maximum error value obtained is 0.9964 at 4 bar pressure. The last error value found for a 30 kDa membrane was 0.0472 at a pressure of 5 bars, while the maximum error value was 0.4365 at a pressure of 4.5 bars. The lowest error value for a 10 kDa membrane is 0.2855 at 9 bars of pressure, while the maximum error value is 0.5734 at 10 bars of pressure. The data was then presented using a graph indicating the relationship between the volume of permeate produced from the experimental data and the time calculation. If the resultant graphs coincide, the filtering equation model is appropriate for use with the data acquired by this inquiry, and CV and Ve values may be computed. Figures 3a, 3b, and 3c show the graph of permeate volume against time acquired on 50 kDa, 30 kDa, and 10 kDa PES membranes following the ultrafiltration technique.

According to the results of utilizing the filtration model equation shown in Figures 3a, 3b, and 3c, this model equation is appropriate for analyzing the link between permeate volume and time. This is proven by the data volume and estimated volume figures, which tend to match. The graph indicates that the larger the filtration rate, the longer the filtration time. This is induced by the development of a cake on the membrane's surface, which restricts filtration and covers the membrane's pores. Based on the batch filtration model created in this work, the model may be used to determine the parameter parameters in ultrafiltration membrane separation to purify proanthocyanidin and other phenolic compounds. It is vital to give attention to the cake formation process on the surface of the membrane to create a better performance with high permeability values and a more precise separation process.

4. CONCLUSION

Experiments and prediction data reveal that the batch filtration model can be used to separate proanthocyanidin compounds from sorghum pericarp extract with similar permeate volume values. As shown by the batch filtration model's SSE values for each MWCO, PES 50 kDa has 0.3855-0.9965, PES 30 kDa has 0.0472-0.4365, and PES 10 kDa has 0.2887-0.5734. Transmembrane pressure and MWCO affect how successfully ultrafiltration membrane technology separates proanthocyanidins. Permeation flow increases with transmembrane pressure, and depending on membrane and fluid, MWCO affects permeability due to bigger membrane holes. Fluids may readily move through membranes with higher MWCO. In addition to accelerating feed flow and overcoming resistance, high transmembrane pressure enhances the buildup of chemicals for protrusion component breakdown, resulting in a blocking mechanism at the membrane surface or pores. According to Hermia's model, the majority of fouling formation mechanisms are caused by the formation of a cake layer on the membrane surface with an R^2 value > 0.99 at each MWCO size of the PES membrane, followed by standard model blocking, intermediate blocking, and complete blocking.

5. ACKNOWLEDGEMENTS

6. NOTATION

1. A = membrane surface area, cm^2
2. t = time, minute
3. J = Fluks, $L/m^2.h$
4. J_0 = Fluks at t =0, $L/m^2.h$
5. V = permeat volume, L
6. n = fouling mechanism value
7. K_c = Hermia's model constant for complete blocking, s^{-1}
8. K_s = Hermia's model constant for standard blocking, m^{-1}
9. K_i = Hermia's model constant for intermediate blocking, $s^{-0.5}m^{-0.5}$
10. K_g = Hermia's model constant for cake layer formation model, $s\ m^{-2}$
11. $\frac{dV}{dt}$ = filtration rate, L/h
12. Cv = filtration constant, cm^2/s
13. Ve = equivalent volume, mL
14. K = permeability
15. ΔPc = pressure drop
16. X = *cake porosity*
17. x = mass fraction of solids in slurry
18. L = cake thickness, cm
19. μ = viscosity, gram/cm.s
20. ρ = density, gram/mL
21. ρs = solids density at *cake,* $gram/cm^3$

REFERENCES

Abolore M, Jami MS, Muyibi SA. 2010. Tertiary treatment of biologically treated palm oil mill effluent (POME) using uf membrane system : Effect of MWCO and transmembrane pressure. 1(2). https://core.ac.uk/pdf/aaa300366 698.pdf.

Afandy MA, Sediawan WB, Hidayat M, Susanti DY. 2023. Purification of proanthocyanidins from the extract of red sorghum pericarp using ultrafiltration membrane. AIP Conference Proceedings. Volume 2623. doi:https://doi.org/10.1063/5.0129732.

Alsvik IL, Hägg MB. 2013. Pressure retarded osmosis and forward osmosis membranes: Materials and methods. Polymers. 5(1):303–327. doi:10.3390/polym5010303.

Ambarita AC, Mulyati S, Arahman N, Bilad MR, Shamsuddin N, Ismail NM. 2021. Improvement of properties and performances of polyethersulfone ultrafiltration membrane by blending with bio-based dragonbloodin resin. Polymers. 13(24). doi:10.3390/polym13244436.

Anderson RC, Vodovnik M, Min BR, Pinchak WE, Krueger NA, Harvey RB, Nisbet DJ. 2012. Bactericidal effect of hydrolysable and condensed tannin extracts on Campylobacter jejuni in vitro. Folia Microbiologica. 57(4):253–258. doi:10.1007/s12223-012-0119-4.

Ang WL, Mohammad AW. 2015. Mathematical modeling of membrane operations for water treatment. Elsevier Ltd. doi:10.1016/B978-1-78242-121-4.00012-5.

Arribas P, Khayet M, García-Payo MC, Gil L. 2015. Novel and emerging membranes for water treatment by hydrostatic pressure and vapor pressure gradient membrane processes. Elsevier Ltd. doi:10.1016/B978-1-78242-121-4.00008-3.

Asif MB, Hai FI, Jegatheesan V, Price WE, Nghiem LD, Yamamoto K. 2018. Applications of membrane bioreactors in biotechnology processes. Elsevier Inc. doi:10.1016/B978-0-12-813606-5.00008-7.

Barros F, Awika J, Rooney LW. 2014. Effect of molecular weight profile of sorghum proanthocyanidins on resistant starch formation. Journal of the Science of Food and Agriculture. 94(6):1212–1217. doi:10.1002/jsfa.6400.

Blandin G, Verliefde AR, Comas J, Rodriguez-Roda I, Le-Clech P. 2016. Efficiently combining water reuse and desalination through forward osmosis-reverse osmosis (FO-RO) hybrids: A critical review. Membranes. 6(3). doi:10.3390/membranes6030037.

Bolton G, LaCasse D, Kuriyel R. 2006. Combined models of membrane fouling: Development and application to microfiltration and ultrafiltration of biological fluids. Jour-

nal of Membrane Science. 277(1-2):75–84. doi:10.1016/j.memsci.2004.12.053.

Cai M, Lv Y, Luo S, Liu Y, Sun P. 2018. Fouling behavior of polyphenols during model juice ultrafiltration: effect of membrane properties. Food and Bioprocess Technology. 11(9):1787–1793. doi:10.1007/s11947-018-2110-9.

Cassano A, Conidi C, Ruby-Figueroa R, Castro-Muñoz R. 2018. Nanofiltration and tight ultrafiltration membranes for the recovery of polyphenols from agro-food by-products. International Journal of Molecular Sciences. 19(2). doi:10.3390/ijms19020351.

Chen X, Qi T, Zhang Y, Wang T, Qiu M, Cui Z, Fan Y. 2020. Facile pore size tuning and characterization of nanoporous ceramic membranes for the purification of polysaccharide. Journal of Membrane Science. 597:117631. doi:10.1016/j.memsci.2019.117631.

Chhabra R, Basavaraj M. 2019. Coulson and Richardson's chemical engineering. sixth edit edition. Volume 2A. Oxford: Butterworth-Heinemann. doi:https://doi.org/10.1016/C2009-0-11215-1.

Chiremba C, Rooney LW, Beta T. 2012. Microwave-assisted extraction of bound phenolic acids in bran and flour fractions from sorghum and maize cultivars varying in hardness. Journal of Agricultural and Food Chemistry. 60(18):4735–4742. doi:10.1021/jf300279t.

Cifuentes-Cabezas M, Bohórquez-Zurita JL, Gil-Herrero S, Vincent-Vela MC, Mendoza-Roca JA, Álvarez-Blanco S. 2023. Deep study on fouling modelling of ultrafiltration membranes used for omw treatment: Comparison between semi-empirical models, response surface, and artificial neural networks. Food and Bioprocess Technology. (0123456789). doi:10.1007/s11947-023-03033-0.

Conidi C, Cassano A, Caiazzo F, Drioli E. 2017. Separation and purification of phenolic compounds from pomegranate juice by ultrafiltration and nanofiltration membranes. Journal of Food Engineering. 195:1–13. doi:10.1016/j.jfoodeng.2016.09.017.

Conidi C, Drioli E, Cassano A. 2018. Membrane-based agro-food production processes for polyphenol separation, purification and concentration. Current Opinion in Food Science. 23:149–164. doi:10.1016/j.cofs.2017.10.009.

Conidi C, Drioli E, Cassano A. 2020. Coupling ultrafiltration-based processes to concentrate phenolic compounds from aqueous goji berry extracts. Molecules. 25(16). doi:10.3390/molecules25163761.

Córdova A, Astudillo C, Illanes A. 2018. Membrane technology for the purification of enzymatically produced oligosaccharides. doi:10.1016/B978-0-12-815056-6.00004-8.

Czochanska Z, Foo LY, Newmann RH, Porter LJ. 1980. Polymeric proanthocyanidins. Stereochemistry, structural units, and molecular weight. Journal of the chemical society. 1:2278–2286. doi:10.1039/P19800002278.

Darunee Bhongsuwan, Tripob Bhongsuwan, Jamras Na-Suwan. 2002. Construction of a dead-end type micro- to R.O. membrane test cell and performance test with the laboratory- made and commercial membranes. Songklanakarin Journal of Science and Technology. 24(Suppl.):999–1007. https://web.archive.org/web/20180425014039id_/http://rdo.psu.ac.th/sjstweb/journal/24-Suppl-1/26reverse-osmosis.pdf.

Dillmann S, Kaushik SA, Stumme J, Ernst M. 2020. Characterization and performance of lbl-coated multibore membranes: Zeta potential, mwco, permeability and sulfate rejection. Membranes. 10(12):1–15. doi:10.3390/membranes10120412.

Dykes L, Rooney LW. 2007. Phenolic compounds in cereal grains and their health benefits. Cereal Foods World. 52(3):105–111. doi:10.1094/CFW-52-3-0105.

Fan G, Su Z, Lin R, Lin X, Xu R, Chen W. 2016. Influence of membrane materials and operational modes on the performance of ultrafiltration modules for drinking water treatment. International Journal of Polymer Science. 2016. doi:10.1155/2016/6895235.

Favre E. 2022. The Future of Membrane Separation Processes: A Prospective Analysis. Frontiers in Chemical Engineering. 4(May):1–5. doi:10.3389/fceng.2022.916054.

Hagerman AE, Butler LG. 1980. Condensed tannin purification and characterization of tannin-associated proteins. Journal of Agricultural and Food Chemistry. 28(5):947–952. doi:10.1021/jf60231a011.

Hori K, Unno H. 2011. Integrated production and separation. second edi edition. Volume 2. Elsevier B.V. doi:10.1016/B978-0-08-088504-9.00116-1.

Koonani H, Amirinejad M. 2019. Combined three mechanisms models for membrane fouling during microfiltration. Journal of Membrane Science and Research. 5(4):274–282. doi:10.22079/jmsr.2019.95781.1224.

Lee SM, Lin JJ, Liao CY, Cheng HL, Sun Pan B. 2014. Phenolic acids identified in sorghum distillery residue demonstrated Antioxidative and anti-cold-stress properties in cultured tilapia, oreochromis mossambicus. Journal of Agricultural and Food Chemistry. 62(20):4618–4624. doi:10.1021/jf500876k.

Liu L, Luo XB, Ding L, Luo SL. 2018. Application of nanotechnology in the removal of heavy metal from water. Elsevier Inc. doi:10.1016/B978-0-12-814837-2.00004-4.

Lutz H. 2010. Ultrafiltration: Fundamentals and engineering. Comprehensive Membrane Science and Engineering. 2:115–139. doi:10.1016/B978-0-08-093250-7.00037-2.

Madrona GS, Terra NM, Filho UC, Magalhães FdS, Cardoso VL, Reis MHM. 2019. Purification of phenolic compounds from genipap (Genipa americana L.) extract by the ultrasound assisted ultrafiltration process. Acta Scientiarum - Technology. 41. doi:10.4025/actascitechnol.v41i1.35571.

Malliga P, Bela RB, Shanmugapriya N. 2019. Conversion of textile effluent wastewater into fertilizer using marine cyanobacteria along with different agricultural waste. 1971. Elsevier Inc. doi:10.1016/B978-0-12-817951-2.00005-5.

Massey AR, Reddivari L, Vanamala J. 2014. The dermal layer of sweet sorghum (sorghum bicolor) stalk, a byproduct of biofuel production and source of unique 3-deoxyanthocyanidins, has more antiproliferative and proapoptotic activity than the pith in p53 Variants of HCT116 and colon cancer stem cel. Journal of Agricultural and Food Chemistry. 62(14):3150–3159. doi:10.1021/jf405415u.

Md Yunos KF, Mazlan NA, Naim MNM, Baharuddin AS, Hassan AR. 2019. Ultrafiltration of palm oil mill effluent: Effects of operational pressure and stirring speed on per-

formance and membranes fouling. Environmental Engineering Research. 24(2):263–270. doi:10.4491/EER.2018.175.

Mejia JA, Ricci A, Figueiredo AS, Versari A, Cassano A, de Pinho MN, Parpinello GP. 2022. Membrane-based Operations for the Fractionation of Polyphenols and Polysaccharides From Winery Sludges. Food and Bioprocess Technology. 15(4):933–948. doi:10.1007/s11947-022-02795-3.

Mora J, Pott DM, Osorio S, Vallarino JG. 2022. Regulation of plant tannin synthesis in crop species. Frontiers in Genetics. 13(May):1–18. doi:10.3389/fgene.2022.870976.

Nawaz H, Shi J, Mittal GS, Kakuda Y. 2006. Extraction of polyphenols from grape seeds and concentration by ultrafiltration. Separation and Purification Technology. 48(2):176–181. doi:10.1016/j.seppur.2005.07.006.

Pabby AK, Rizvi SSH, Sastre AM, Press CRC. 2009. Handbook of membrane separations chemical, pharmaceutical, food, and biotechnological applications. doi:https://doi.org/10.1201/9781420009484.

Pinto PR, Mota IF, Pereira CM, Ribeiro AM, Loureiro JM, Rodrigues AE. 2017. Separation and recovery of polyphenols and carbohydrates from Eucalyptus bark extract by ultrafiltration/diafiltration and adsorption processes. Separation and Purification Technology. 183:96–105. doi:10.1016/j.seppur.2017.04.003.

Purwayantie S, Sediawan WB. 2020. Membrane separation for recovery of umami compounds: Review of current and recently developed membranes. Journal of Environmental Treatment Techniques. 8(1):390–402. https://www.dormaj.com.

Rahimpour A, Madaeni SS, Mehdipour-Ataei S. 2008. Synthesis of a novel poly(amide-imide) (PAI) and preparation and characterization of PAI blended polyethersulfone (PES) membranes. Journal of Membrane Science. 311(1-2):349–359. doi:10.1016/j.memsci.2007.12.038.

Rai P, Majumdar GC, Sharma G, Das Gupta S, De S. 2006. Effect of various cutoff membranes on permeate flux and quality during filtration of Mosambi (Citrus sinensis (L.) Osbeck) juice. Food and Bioproducts Processing. 84(3C):213–219. doi:10.1205/fbp.05181.

Rajendran SR, Mason B, Doucette AA. 2021. Review of membrane separation models and technologies: processing complex food-based biomolecular fractions. Food and Bioprocess Technology. 14(3):415–428. doi:10.1007/s11947-020-02559-x.

Ramli R, Bolong N. 2016. Effects of pressure and temperature on ultrafiltration hollow fiber membrane in mobile water treatment system. Journal of Engineering Science and Technology. 11(7):1031–1040. https://jestec.taylors.edu.my/Vol11issue7July2016/11_7_9.pdf.

Ratnavathi CV, Tonapi VA. 2021. Functional characteristics and nutraceuticals of grain sorghum. Sorghum in the 21st Century: Food - Fodder - Feed - Fuel for a Rapidly Changing World:839–858. doi:10.1007/978-981-15-8249-3_33.

Rauf A, Imran M, Abu-Izneid T, Iahtisham-Ul-Haq, Patel S, Pan X, Naz S, Sanches Silva A, Saeed F, Rasul Suleria HA. 2019. Proanthocyanidins: A comprehensive review. Biomedicine and Pharmacotherapy. 116(May). doi:10.1016/j.biopha.2019.108999.

Raza W, Lee J, Raza N, Luo Y, Kim KH, Yang J. 2019. Removal of phenolic compounds from industrial waste water based on membrane-based technologies. Journal of Industrial and Engineering Chemistry. 71:1–18. doi:10.1016/j.jiec.2018.11.024.

Rodrigues RP, Gando-Ferreira LM, Quina MJ. 2020. Micellar enhanced ultrafiltration for the valorization of phenolic compounds and polysaccharides from winery wastewaters. Journal of Water Process Engineering. 38(May):101565. doi:10.1016/j.jwpe.2020.101565.

Sadr SM, Saroj DP. 2015. Membrane technologies for municipal wastewater treatment. Elsevier Ltd. doi:10.1016/B978-1-78242-121-4.00014-9.

Saleh TA, Gupta VK. 2016. An overview of membrane science and technology. Nanomaterial and Polymer Membranes:1–23. doi:10.1016/b978-0-12-804703-3.00001-2.

Stefoska-Needham A, Beck EJ, Johnson SK, Tapsell LC. 2015. Sorghum: An Underutilized Cereal Whole Grain with the Potential to Assist in the Prevention of Chronic Disease. Food Reviews International. 31(4):401–437. doi:10.1080/87559129.2015.1022832.

Susanti DY, Sediawan WB, Fahrurrozi M, Hidayat M, Putri AY. 2021. Encapsulation of red sorghum extract rich in proanthocyanidins: Process formulation and mechanistic model of foam-mat drying at various temperature. Chemical Engineering and Processing - Process Intensification. 164(March):108375. doi:10.1016/j.cep.2021.108375.

Svensson L, Sekwati-Monang B, Lutz DL, Schieber R, Gänzle MG. 2010. Phenolic acids and flavonoids in nonfermented and fermented red sorghum (Sorghum bicolor (L.) Moench). Journal of Agricultural and Food Chemistry. 58(16):9214–9220. doi:10.1021/jf101504v.

Syahputri GA, Santoso U, Supriyanto. 2021. Ultrafiltration for the separation of polyphenol oxidase and peroxidase and its effect on physicochemical and antioxidant properties of coconut (Cocos nucifera l.) water. Food Research. 5(4):163–172. doi:10.26656/fr.2017.5(4).013.

Vela MCV, Blanco SÁ, García JL, Rodríguez EB. 2008. Analysis of membrane pore blocking models applied to the ultrafiltration of PEG. Separation and Purification Technology. 62(3):489–498. doi:10.1016/j.seppur.2008.02.028.

Víctor-Ortega MD, Martins RC, Gando-Ferreira LM, Quinta-Ferreira RM. 2017. Recovery of phenolic compounds from wastewaters through micellar enhanced ultrafiltration. Colloids and Surfaces A: Physicochemical and Engineering Aspects. 531(May):18–24. doi:10.1016/j.colsurfa.2017.07.080.

Wang Z, Wang H, Liu J, Zhang Y. 2014. Preparation and antifouling property of polyethersulfone ultrafiltration hybrid membrane containing halloysite nanotubes grafted with MPC via RATRP method. Desalination. 344:313–320. doi:10.1016/j.desal.2014.03.040.

Wen X, He C, Hai Y, Ma R, Sun J, Yang X, Qi Y, Wei H, Chen J. 2022. Fabrication of an antifouling PES ultrafiltration membrane: Via blending SPSF. RSC Advances. 12(3):1460–1470. doi:10.1039/d1ra06354e.

Wu G, Bornman JF, Bennett SJ, Clarke MW, Fang Z, Johnson SK. 2017. Individual polyphenolic profiles and antioxidant activity in sorghum grains are influenced by very

low and high solar UV radiation and genotype. Journal of Cereal Science. 77:17–23. doi:10.1016/j.jcs.2017.07.014.

Wu Y, Li X, Xiang W, Zhu C, Lin Z, Wu Y, Li J, Pandravada S, Ridder DD, Bai G, Wang ML, Trick HN, Beane SR, Tuinstra MR, Tesso TT, Yu J. 2012. Presence of tannins in sorghum grains is conditioned by different natural alleles of Tannin1. Proceedings of the National Academy of Sciences of the United States of America. 109(26):10281–10286. doi: 10.1073/pnas.1201700109.

Zheng L, Su Y, Wang L, Jiang Z. 2009. Adsorption and recovery of methylene blue from aqueous solution through ultrafiltration technique. Separation and Purification Technology. 68(2):244–249. doi:10.1016/j.seppur.2009.05.010.

Zhu Z, Liu Y, Guan Q, He J, Liu G, Li S, Ding L, Jaffrin MY. 2015. Purification of purple sweet potato extract by dead-end filtration and investigation of membrane fouling mechanism. Food and Bioprocess Technology. 8(8):1680–1689. doi:10.1007/s11947-015-1532-x.